

1 Appendix: Supplementary Materials for Explainer-Explained Architecture for 2 Vision Models

3 1 EVALUATION METRICS

4 There is no single measure or test set which is generally acceptable for evaluating explanation maps. Hence, in order to ensure comparability,
 5 the evaluations in this research follow earlier works [2–4, 6]. In general, the various tests entail different types of masking of the original
 6 input according to the explanation maps and investigating the change in the model’s prediction for the masked input compared to its original
 7 prediction based on the unmasked input. There are two variants for these tests which differ based on the class of reference. In one variant,
 8 the difference in predictions refers to the ground-truth class, and in the second variant, the difference in predictions refers to the model’s
 9 original top-predicted class. In the manuscript, we report results for both variants and dub the first variant as ‘target’ and the second variant
 10 as ‘predicted’, respectively.

11 In what follows, we list and define the different evaluation measures used in this research:

12 (1) Average Drop Percentage (**ADP**) [2]: $ADP = 100\% \cdot \frac{1}{N} \sum_{i=1}^N \frac{\max(0, Y_i^c - O_i^c)}{Y_i^c}$, where N is the total number of images in the evaluated
 13 dataset, Y_i^c is the model’s output score (confidence) for class c w.r.t. the original image i . O_i^c is the same model’s score, this time w.r.t.
 14 to a masked version of the original image (produced by the Hadamard product of the original image with the explanation map). For
 15 **ADP lower** values indicate better results.

16 (2) Percentage of Increase in Confidence (**PIC**) [2]: $PIC = 100\% \cdot \frac{1}{N} \sum_{i=1}^N \mathbb{1}(Y_i^c < O_i^c)$. PIC reports the percentage of cases in which the
 17 model’s output scores increase due to the replacement of the original image with the masked version based on the explanation map.
 18 The explanation map is expected to mask the background and help the model to focus on the original image. Hence, in PIC **higher**
 19 values indicate a better result.

20 (3) Perturbation tests entail a stepwise process in which pixels in the original image are gradually masked out according to their
 21 relevance score obtained from the explanation map [4]. At each step, an additional 10% of the pixels are removed and the original
 22 image is gradually blacked out. The performance of the explanation model is assessed by measuring the area under the curve (AUC)
 23 with respect to the model’s prediction on the masked image compared to its prediction with respect to the original (unmasked)
 24 image. In perturbation tests [4], for each image, we first extract an explanation map based on the specific explanation method. Then,
 25 we gradually mask out pixels of the input image and measure the mean top-1 accuracy of the network. We consider two types of
 26 masking:
 27

28 (a) Positive perturbation (**POS**), in which we mask the pixels in decreasing order, from the highest relevance to the lowest, and
 29 expect to see a steep decrease in performance, indicating that the masked pixels are important to the classification score. Hence,
 30 for the POS perturbation test, lower values indicate better performance.

31 (b) Negative perturbation (**NEG**), in which we mask the pixels in increasing order, from lowest to highest. A good explanation
 32 would maintain the accuracy of the model while removing pixels that are not related to the class of interest. Hence, for the NEG
 33 perturbation test, lower values indicate better performance.

34 In both positive and negative perturbations, we measure the area-under-the-curve (AUC), for erasing between 10%-90% of the pixels.

35 As explained above, results are reported with respect to the ‘predicted’ or the ‘target’ (ground-truth) class.

36 (4) The deletion and insertion metrics [6] are described as follows:

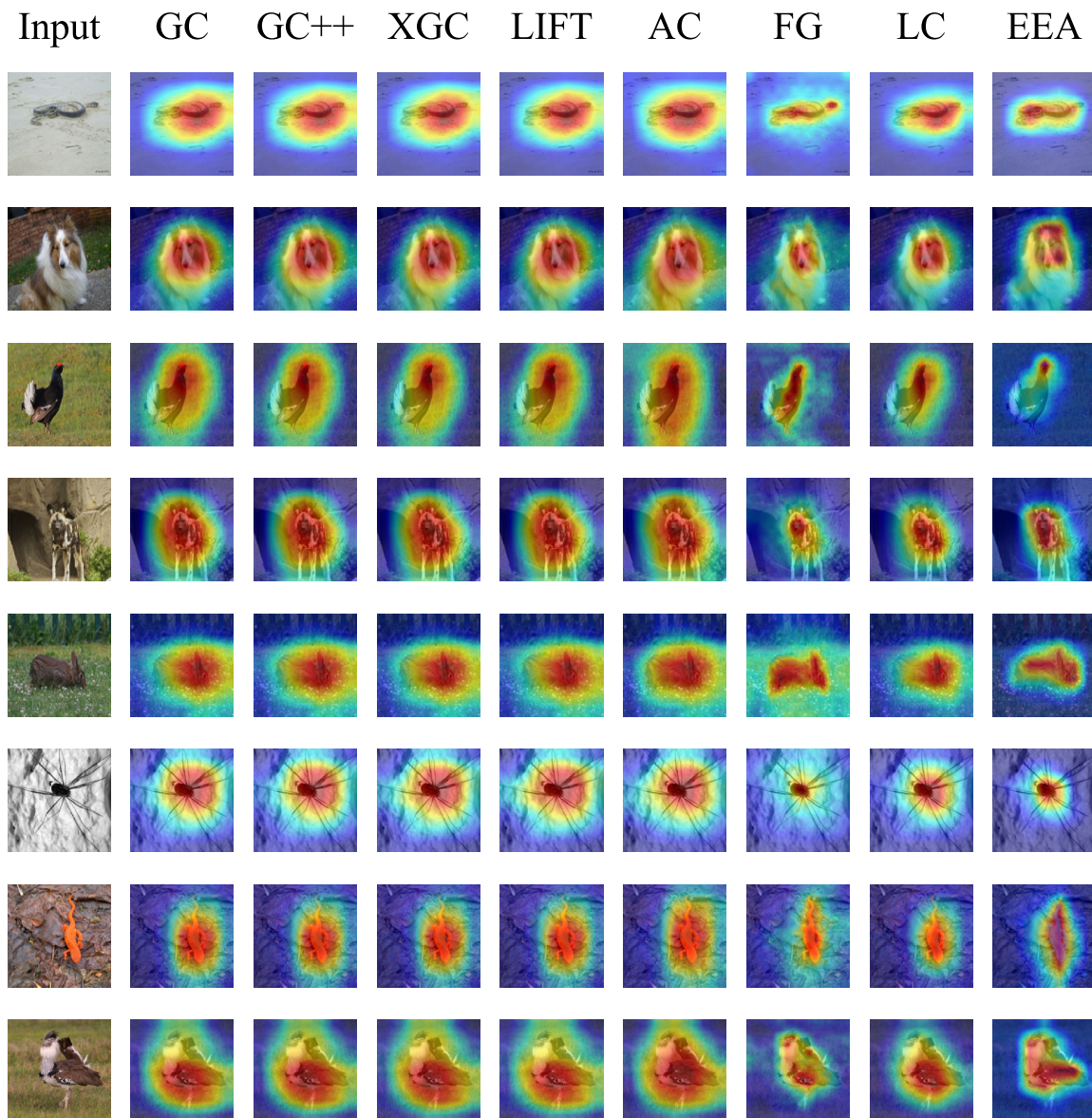
37 (a) The deletion (**DEL**) metric measures a decrease in the probability of the class of interest as more and more important pixels are
 38 removed, where the importance of each pixel is obtained from the generated explanation map. A sharp drop and thus a low area
 39 under the probability curve (as a function of the fraction of removed pixels) means a good explanation.

40 (b) In contrast, the insertion (**INS**) metric measures the increase in probability as more and more pixels are revealed, with higher
 41 AUC indicative of a better explanation.

42 Note that there are several ways in which pixels can be removed from an image [5]. In this work, we remove pixels by setting their
 43 value to zero. Gradual removal or introduction of pixels is performed in steps of 0.1 i.e., remove or introduce 10% of the pixels on
 44 each step.

117 2 EEA FOR CNNS

118 In continuation of our discussion of EEA for CNN models, we present visual comparisons in Fig. 1 of the different CNN explanation baselines
 119 using a random sample of images from Imagenet's validation set. The examples provided demonstrate the effectiveness of EEA's explanation
 120 maps in accurately identifying and highlighting relevant objects in the image. Conversely, Grad-CAM's (GC) explanation maps are generally
 121 larger and cover a greater area, which may explain their superior performance in the ADP and PIC tests as presented in Table 5. By capturing
 122 a larger area around the object, Grad-CAM is able to maintain more relevant information in the masked image, which aids its performance
 123 in these tests. However, it is important to note that the ADP test can be problematic, as a simple all-ones mask (that effectively leaves the
 124 image unmasked) can yield an optimal ADP value of 0. Despite Grad-CAM's success in these tests, the masks generated by this method are
 125 considerably less focused on the object, as illustrated in Fig. 1.
 126



168 **Figure 1: Sample images from ImageNet validation set for CNN models. Image classes are listed according to their row-wise**
 169 **appearance: “sea snake”, “shetland sheepdog”, “black grouse”, “african hunting dog”, “wood rabbit”, “daddy longlegs”, “eft”,**
 170 **“bustard”.**

171
 172
 173
 174
 175
 176
 177
 178
 179
 180
 181
 182
 183
 184
 185
 186
 187
 188
 189
 190
 191
 192
 193
 194
 195
 196
 197
 198
 199
 200
 201
 202
 203
 204
 205
 206
 207
 208
 209
 210
 211
 212
 213
 214
 215
 216
 217
 218
 219
 220
 221
 222
 223
 224
 225
 226
 227
 228
 229
 230
 231
 232

233 3 SANITY CHECKS FOR SALIENCY MAPS 291

234 As follow to what described in 4.6, this section expands upon the sensitivity tests of EEA. It elucidates with qualitative results to enhance the
 235 reader's understanding of sanity checks. We conducted both the *parameter randomization* and *data randomization* sanity tests as proposed
 236 by [1]. Fig. 8 demonstrates the parameters randomization and data randomization tests in the third and fourth columns, respectively, for a
 237 random sample of images (presented in the first column). We observe that the explanation maps resulting from either data or parameter
 238 randomization significantly differ from the original explanation map produced by EEA (second column). This finding indicates that EEA is
 239 sensitive to both data and parameter randomization, which is a desired property for any explanation method [1].
 240

241 3.1 Parameter Randomization Test 299

242 The parameter randomization test involves a comparison of the explanation maps generated by an explanation method using two distinct
 243 configurations of the same model architecture: (1) the trained setup, where the model is trained on a specific dataset (e.g., a pretrained
 244 vit-base-patch16-224 model trained on ImageNet), and (2) the random setup, which entails the same model architecture but with random
 245 weights (e.g., a vit model initialized with random attention weights). For explanation methods that depend on the specific characteristics of
 246 the model being explained, substantial disparities are expected between the explanation maps produced for the trained model and those
 247 generated for the random model. Conversely, if the explanation maps exhibit similarity, it indicates that the explanation method is insensitive
 248 to the model's parameters, suggesting limited usefulness in terms of explaining and debugging the model.
 249

250 Given a trained model, we consider two types of parameter randomization tests: The first test randomly re-initializes all weights of the
 251 model in a cascading fashion (layer after layer). The second test independently randomizes one layer at a time, while keeping all other layers
 252 fixed. In both cases, we compare the resulting explanations obtained by using the model with random weights to those derived from the
 253 original weights of the model.

254 *Cascading Randomization.* The cascading randomization method involves the randomization of a model's weights, starting from the top
 255 layer and successively moving down to the bottom layer. This process leads to the destruction of the learned weights from the top to the
 256 bottom layers. Figure 2 presents the Spearman correlation (averaged on 50K examples) between the original explanation map obtained by
 257 EEA using the original ViT model (pretrained vit-base-patch16-224) and the explanation map obtained by EEA based cascade randomization
 258 of the original ViT model. ViT-base model uses a 12 layers of attention mechanisms. The markers on the x-axis are between '1' and '13'
 259 (total of 12 layers) where $x = k$ means that the weights of the last k layers of the model are randomized. At $x = 1$ there is no randomization,
 260 hence the correlation with the original model is perfect. Starting from $x = 2$ and up to $x = 13$, the graph depicts a progressive cascade
 261 randomization of the original model. We observe that as more layers' weights are randomized, the correlation with the explanation map of
 262 the original model significantly deteriorates. This behavior showcases the sensitivity of EEA to the model's parameters - an expected and
 263 desired property for any explanation method [1].

264 Figure 3 displays a representative example of explanation maps (bottom) and their overlay to the original image (top), illustrating the
 265 cascading randomization process. The first column presents explanation maps produced by EEA and the original model, while the rest of the
 266 columns present explanation maps produced by EEA and cascading randomized models, where the number i above each column indicates
 267 that the explanation map is produced by a model in which the weights of the last i layers were randomized. It is evident that the quality of
 268 produced explanation maps significantly degrades as more and more layers are set with random weights.
 269

270 *Independent Randomization.* We further consider another version of the model's parameters randomization test, in which a layer-by-layer
 271 randomization is employed, one layer at a time. In this test, we aim to isolate the influence of the randomization of each layer, hence
 272 randomization is applied to one layer's weights at a time, while all other layers' weights are kept identical to their values in the original
 273 model. This randomization methodology enables comprehensive evaluation of the sensitivity of the explanation maps w.r.t. each of the
 274 model's layers.

275 Figure 4 presents results for the independent randomization tests. At $x = 1$ no randomization was applied and the correlation to the
 276 original model is perfect. For $x = i$ ($i > 1$) the graph indicates the correlation of the original model with a model in which only the weights
 277 (attention scores) of the i -th layer were randomized while the weights of all other layers were kept untouched. We observe that the correlation
 278 values are low across all layers which indicates EEA's sensitivity to weight randomization in each layer separately. This property is a desired
 279 property for an explanation method, as it indicates the method's sensitivity to each of the model's layers, independently. Finally, Fig. 5
 280 presents a qualitative example in the same fashion as Fig. 3, this time for the independent randomization test. We observe that the quality of
 281 all explanation maps produced by a randomized version of the model differs significantly from the original explanation map. We conclude
 282 that IIG successfully passes both types of parameter randomization tests.

283 3.2 Data Randomization Test 341

284 The data randomization test is a statistical method used to test the sensitivity of the explanation method to the labeling of the training data.
 285 It is carried out by producing two explanation maps using an identical architecture but with two different datasets: one with the original
 286 labels and another with randomly permuted labels. A desired result for this experiment is obtained when the model proves to be sensitive
 287 to the labeling of the dataset i.e., the produced explanation maps differ significantly between the two cases. However, if the method is
 288 insensitive to the permuted labels, it indicates that the model does not depend on the relationship between instances and labels that exists in
 289

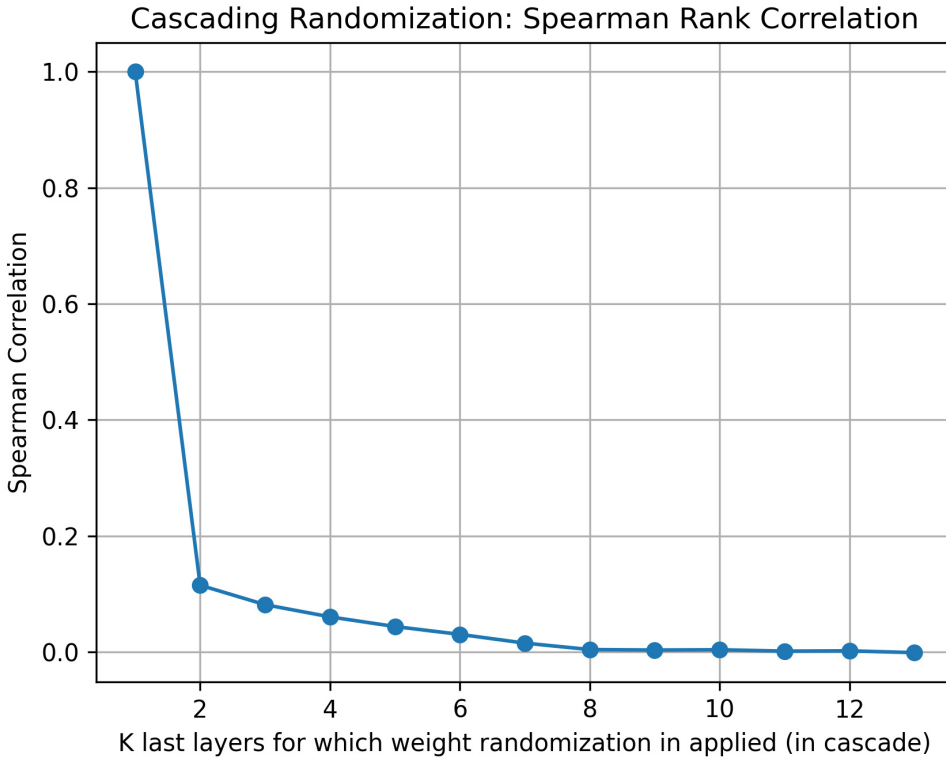


Figure 2: Cascading Randomization: The ViT model (trained on ImageNet dataset) is subjected to successive weights randomization (attention scores), beginning from the last model’s layers to the first ones. The presented graph depicts the Spearman rank correlation (averaged on 50K examples) between the explanation produced by EEA using the original and randomized model’s weights. The x-axis corresponds to the number of layers being randomized, starting from the output layer. The first dot ($x=1$) corresponds to no randomization (the original model is used), hence the correlation between the explanation maps is perfect. See Sec. 3.1 for further details.

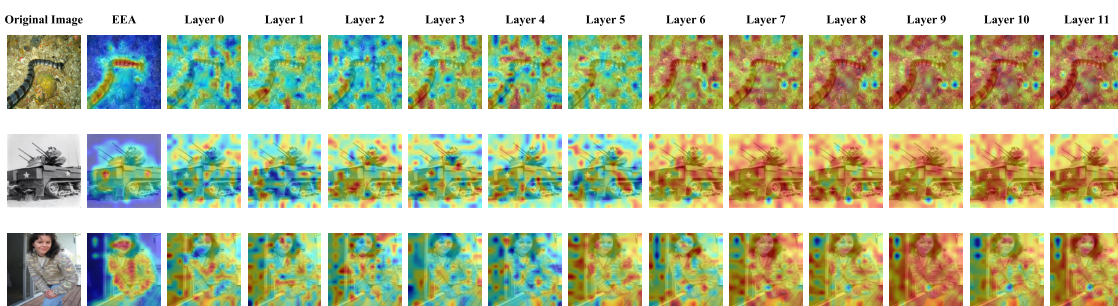


Figure 3: Cascading Randomization on EEA based on random weighted ViT model: The figure presents an original explanations progression from left to right depicts the gradual randomization of network weights up to the layer number depicted at the top of the column (starting from the last layer). See Sec. 3.1 for further details. Image classes according to their row-wise appearance: “sea snake”, “half-track”, “cardigan”.

the original data. To conduct the data randomization test, we permute the training labels in the dataset and train a ViT model to achieve a

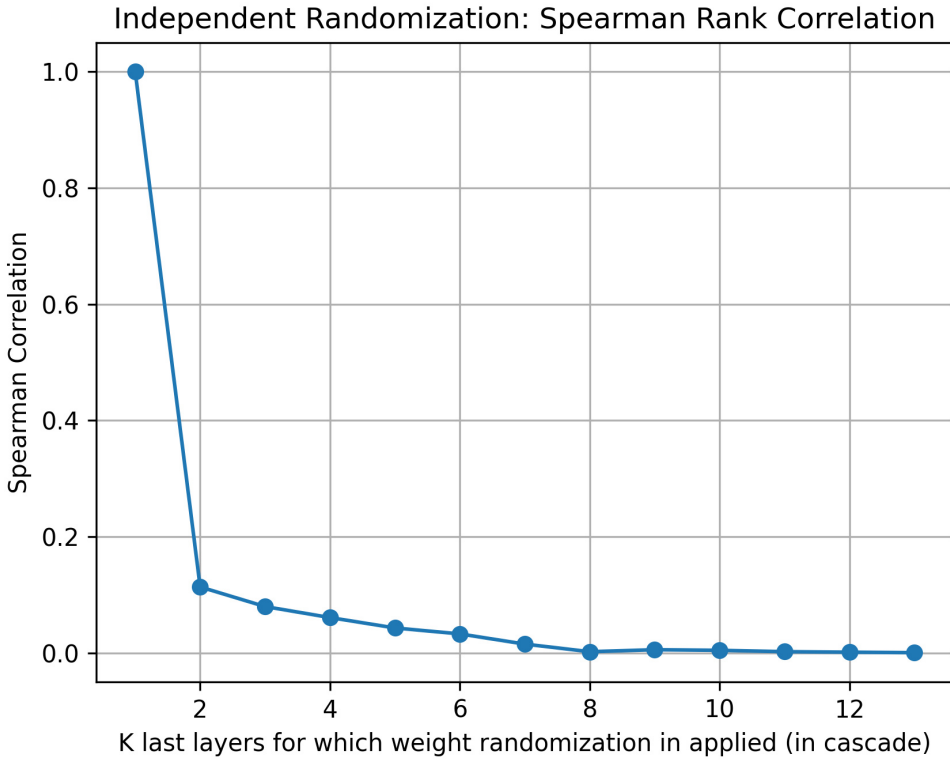


Figure 4: Independent Randomization: The randomization process is carried out independently for each layer of the model, while the remaining weights are retained at their pretrained values. The y-axis of the presented graph represents the rank correlation between the original and randomized explanations, with each point on the x-axis corresponding to a specific layer of the model.

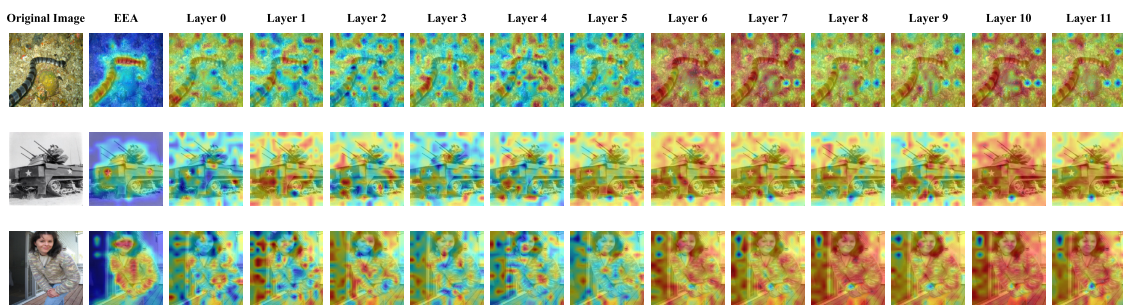


Figure 5: Independent Randomization on EEA based on random weighted ViT model: Similar to Fig. 3, however, this time, each specific layer is randomized independently, while the rest of the weights are kept at their pretrained values. Image classes according to their row-wise appearance: “sea snake”, “half-track”, “cardigan”.

training set accuracy greater than 95%. Note that the resulting model’s test accuracy is never better than randomly guessing a label. We then compute explanations on the same test inputs for both the model trained on true labels and the model trained on randomly permuted labels. Figure 6 presents a box plot computed for the Spearman correlation values obtained for paired explanation maps (50K examples): one produced using the original model that is trained with the ground truth, and another produced by the model trained with the permuted

581 labels. Figure 7 compares visually EEA using the original labels (column 2) and using the randomly permuted labels (column 3). We can
 582 see that the correlation values are very low indicating EEA's sensitivity to the labeling of the training data. Hence, we conclude that EEA
 583 successfully passes the data randomization test.
 584

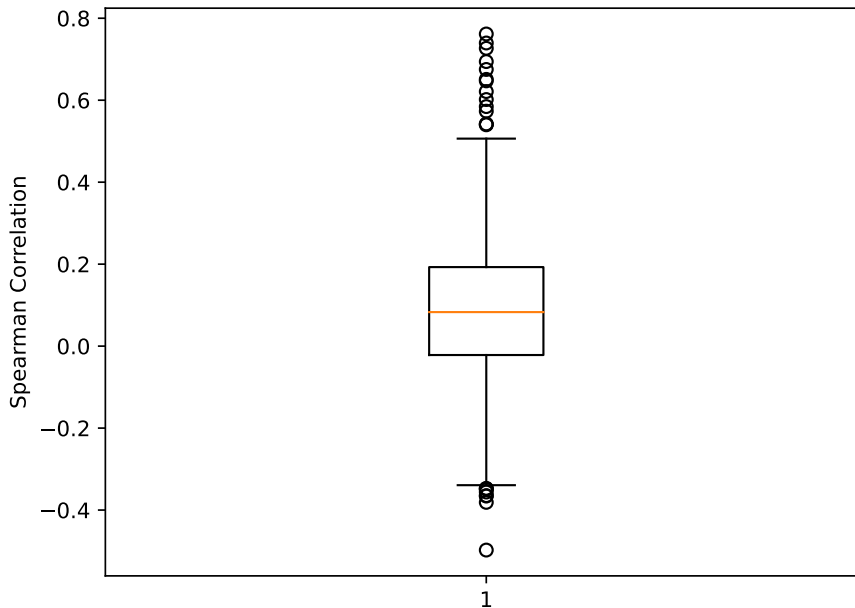


Figure 6: Data Randomization Test: Spearman rank correlation box plot for EEA with the ViT model.

611 Finally, Figure 8 provides supplementary qualitative illustrations for both tests using a pretrained vit-base-patch16-224 model. The EEA
 612 column presents the EEA map which are coherent explanation maps focused on key regions for the classification task. In contrast, in
 613 the last two columns, we see the results following parameter randomization and data randomization. As can be seen, after each type of
 614 randomization, the explanation maps become irrelevant.
 615

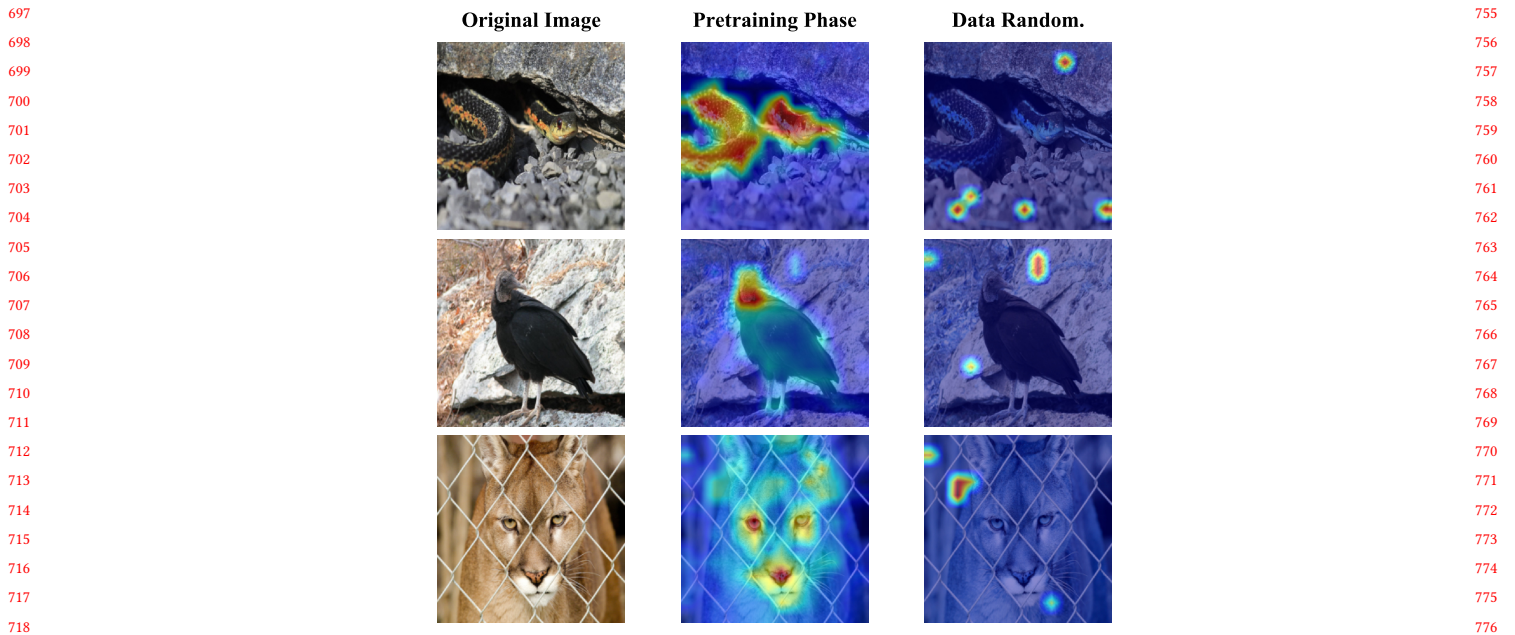


Figure 7: Data Randomization Test: A comparison between original image, EEA and EEA using a random labeled model. Top-to-bottom: “grass snake”, “couga”, “vulture”.

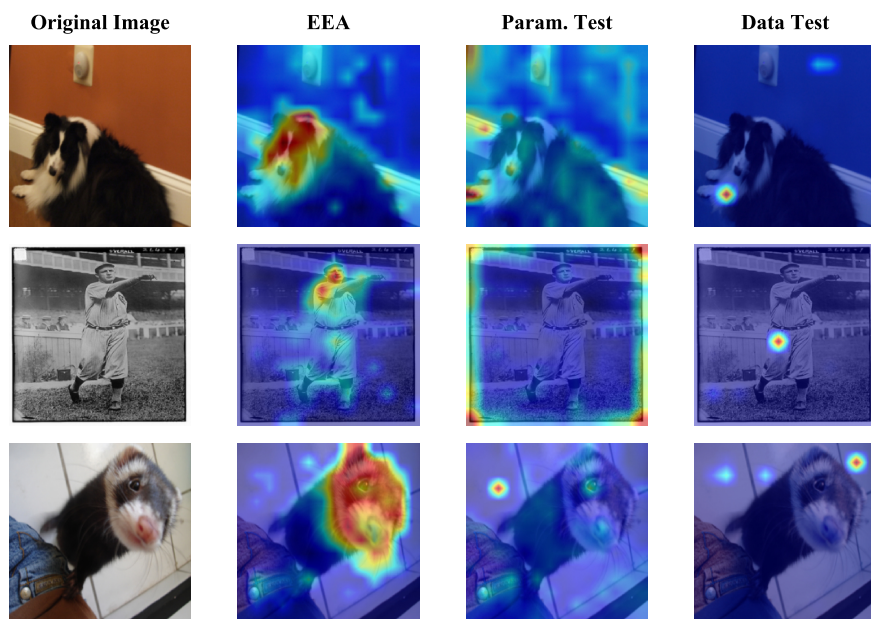


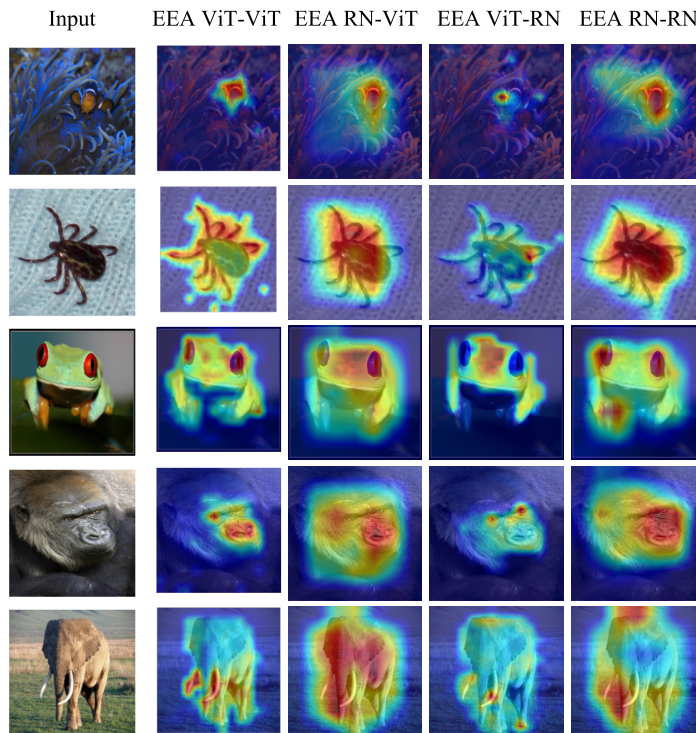
Figure 8: Sanity checks exemplified. Columns 3 and 4 present the explanation maps produced after *parameter randomization* and *data randomization*, respectively. See Sec. 3 for further details. Image classes according to their row-wise appearance: “Shetland sheepdog”, “ballplayer”, “Mustela putorius”.

697
698
699
700
701
702
703
704
705
706
707
708
709
710
711
712
713
714
715
716
717
718
719
720
721
722
723
724
725
726
727
728
729
730
731
732
733
734
735
736
737
738
739
740
741
742
743
744
745
746
747
748
749
750
751
752
753
754

755
756
757
758
759
760
761
762
763
764
765
766
767
768
769
770
771
772
773
774
775
776
777
778
779
780
781
782
783
784
785
786
787
788
789
790
791
792
793
794
795
796
797
798
799
800
801
802
803
804
805
806
807
808
809
810
811
812

813 4 EEA WITH MIXED ARCHITECTURES

814 In our paper, we choose to implement the explainer using the same architecture as the explained model. Choosing the same architecture, and
 815 starting from pretrained weights, simplifies the learning task of the explainer. However, the EEA framework is very general and agnostic
 816 to the explainer's architecture. In order to highlight this point, in Fig 9 we present qualitative examples for different combinations of
 817 explainer-explained architectures, using ViT-B and ResNet. As can be seen, even with mixed architectures the EEA manages to produce
 818 meaningful explanation maps that capture the object of interest in all setups. This showcases the generic nature of the EEA approach which
 819 can be utilized using different architectures. As can be seen, it is possible for the explainer model to utilize a different architecture from that
 820 of the explained model.



848 **Figure 9: Qualitative examples for all possible combinations of explainer-explained architectures, using ViT-B and ResNet.**

851 5 ADDITIONAL EXAMPLES - MULTIPLE-CLASS IMAGES

852 Figure 10 presents additional examples for images that combine two classes of interest. We can see that EEA provides the most accurate
 853 class-specific explanation maps.

855 6 ADDITIONAL EXAMPLES - SINGLE-CLASS IMAGES

857 Figures 11-16 present further comparative examples for explanation maps produced by EEA and the other explanation methods. These
 858 images further demonstrate EEA's advantage over its alternatives.

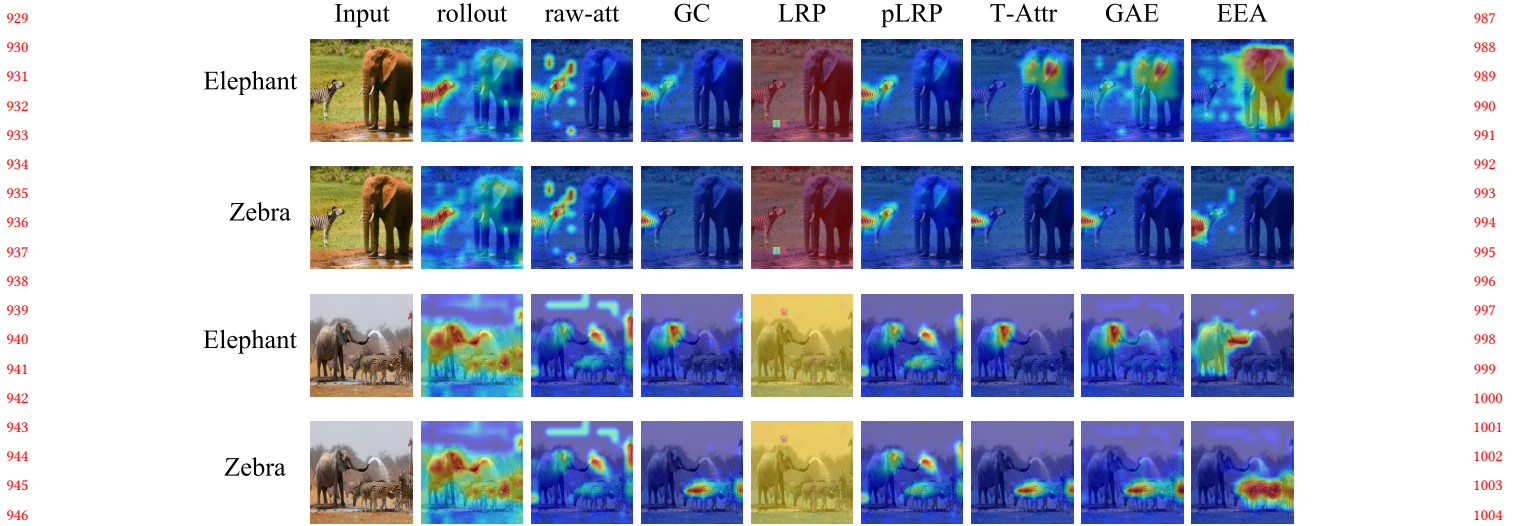
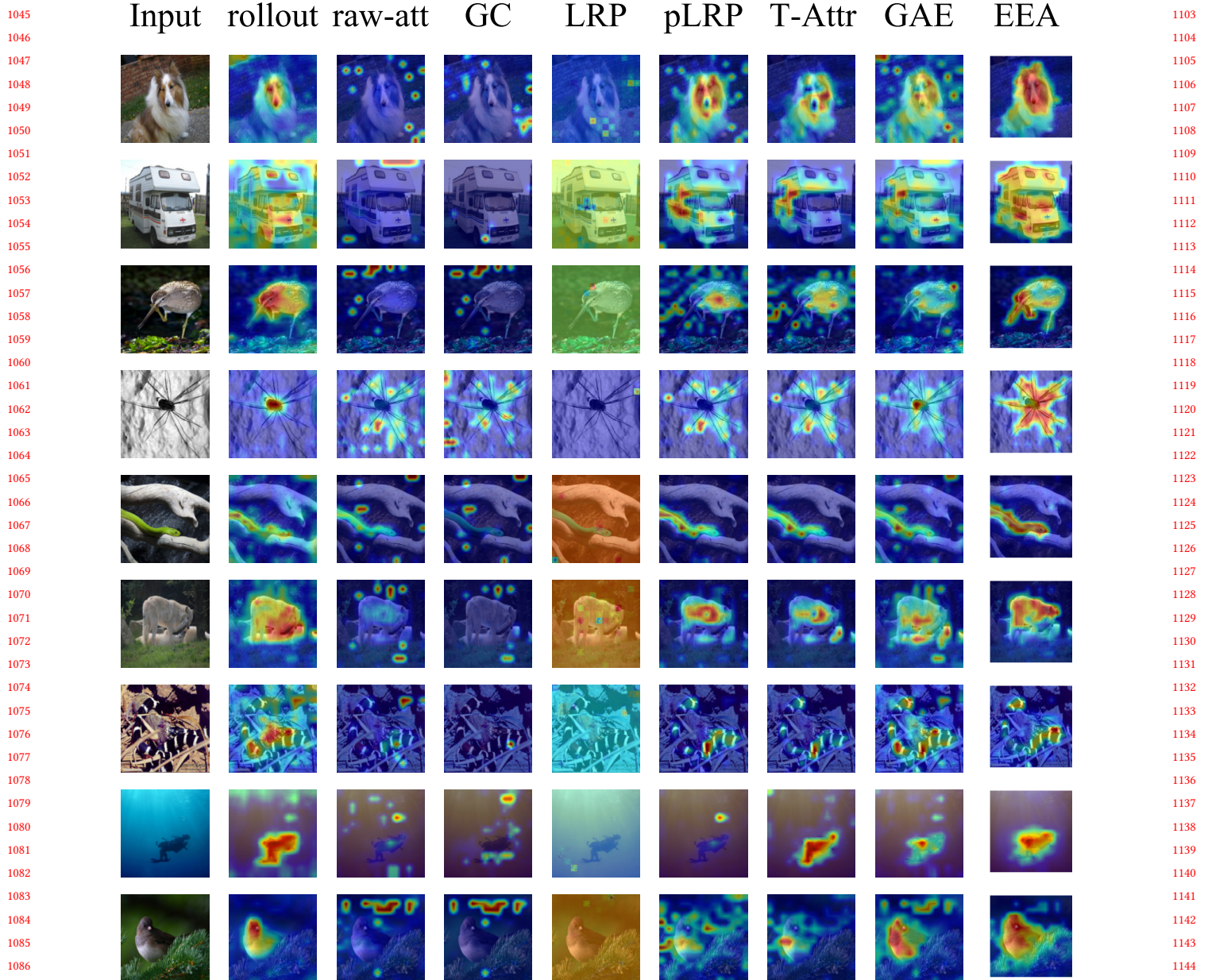
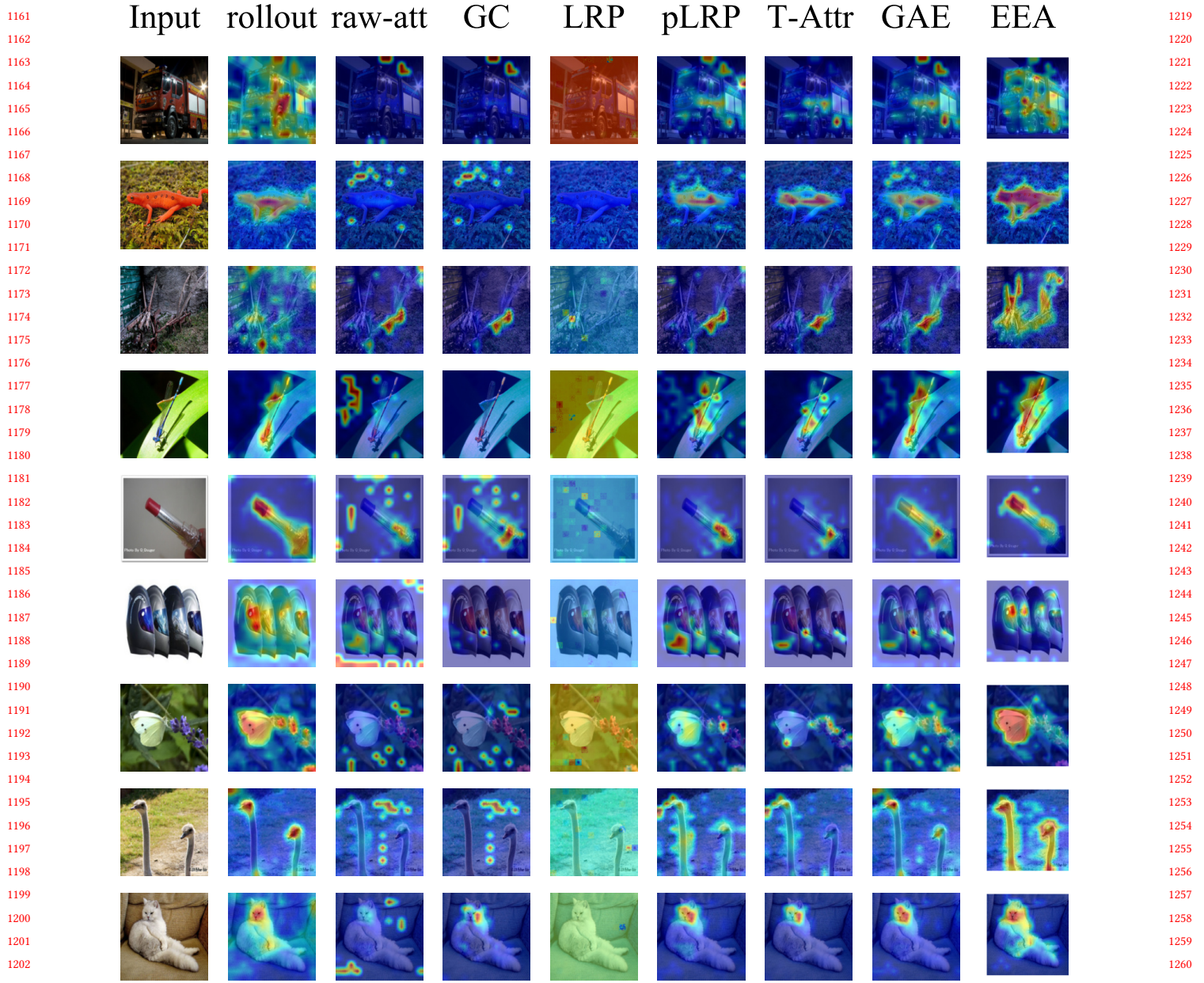
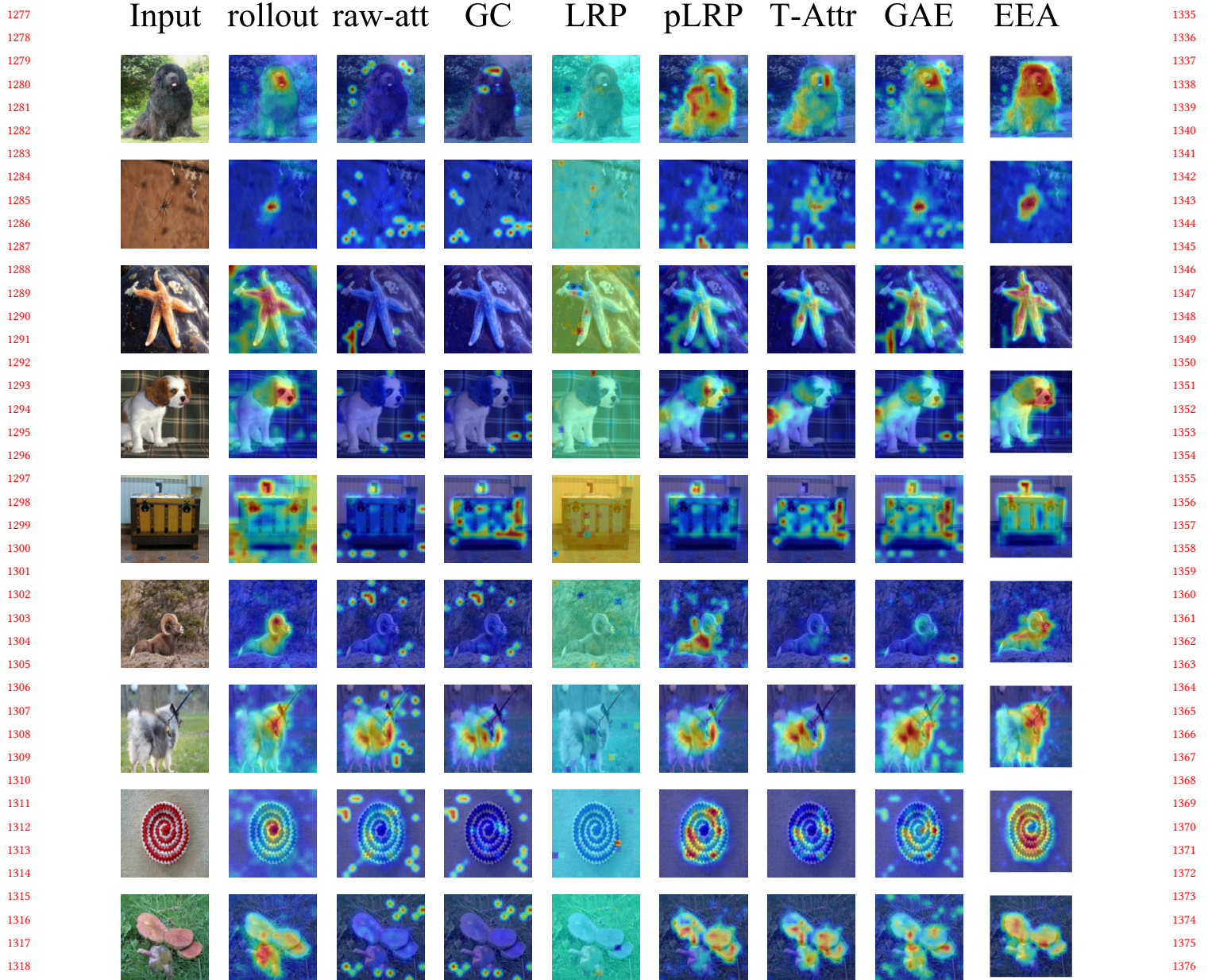


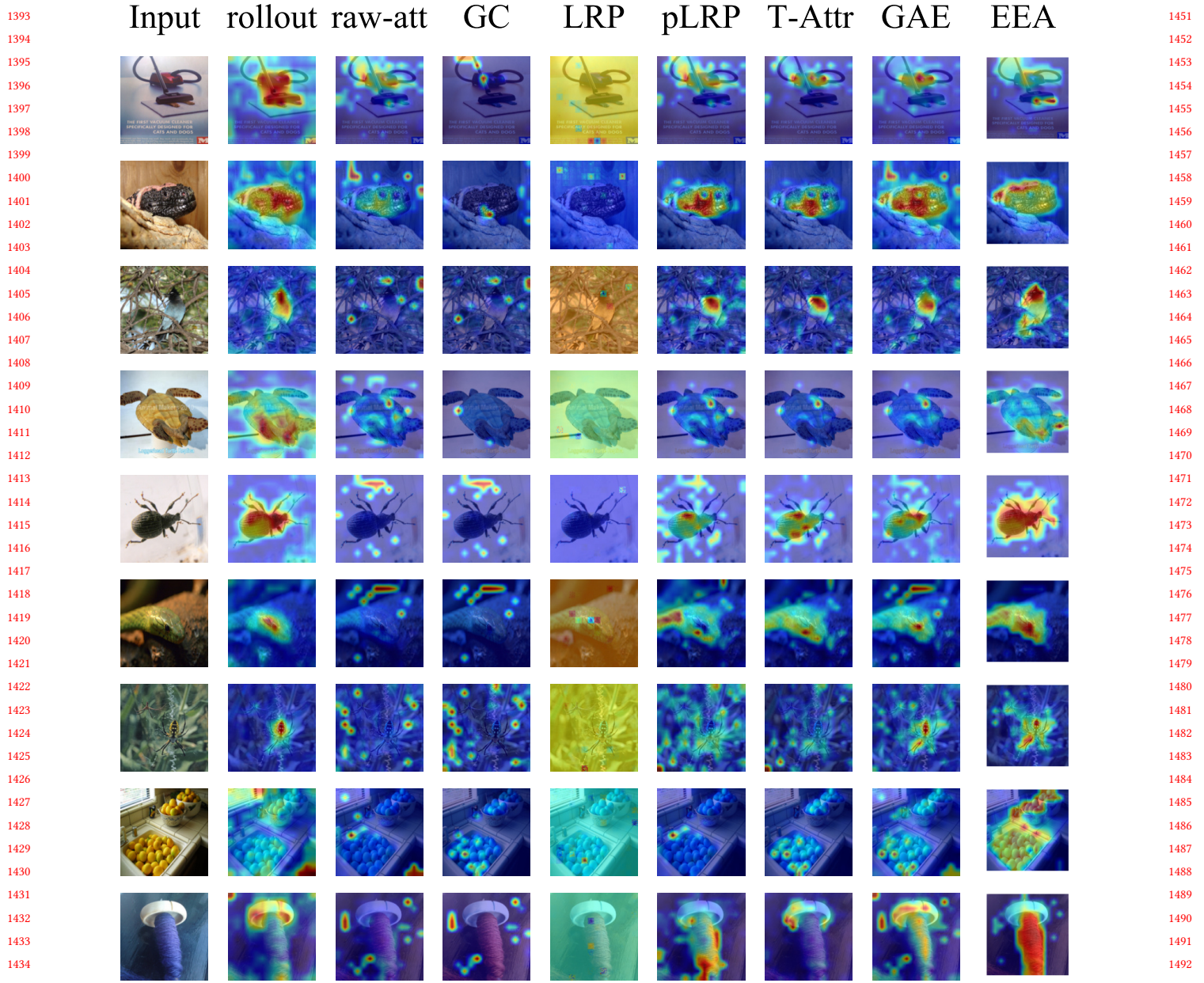
Figure 10: Class-specific visualizations for ViT models. Only GC, T-Attr, GAE, and EEA (this paper) produce class-specific maps, and EEA captures the objects most accurately.

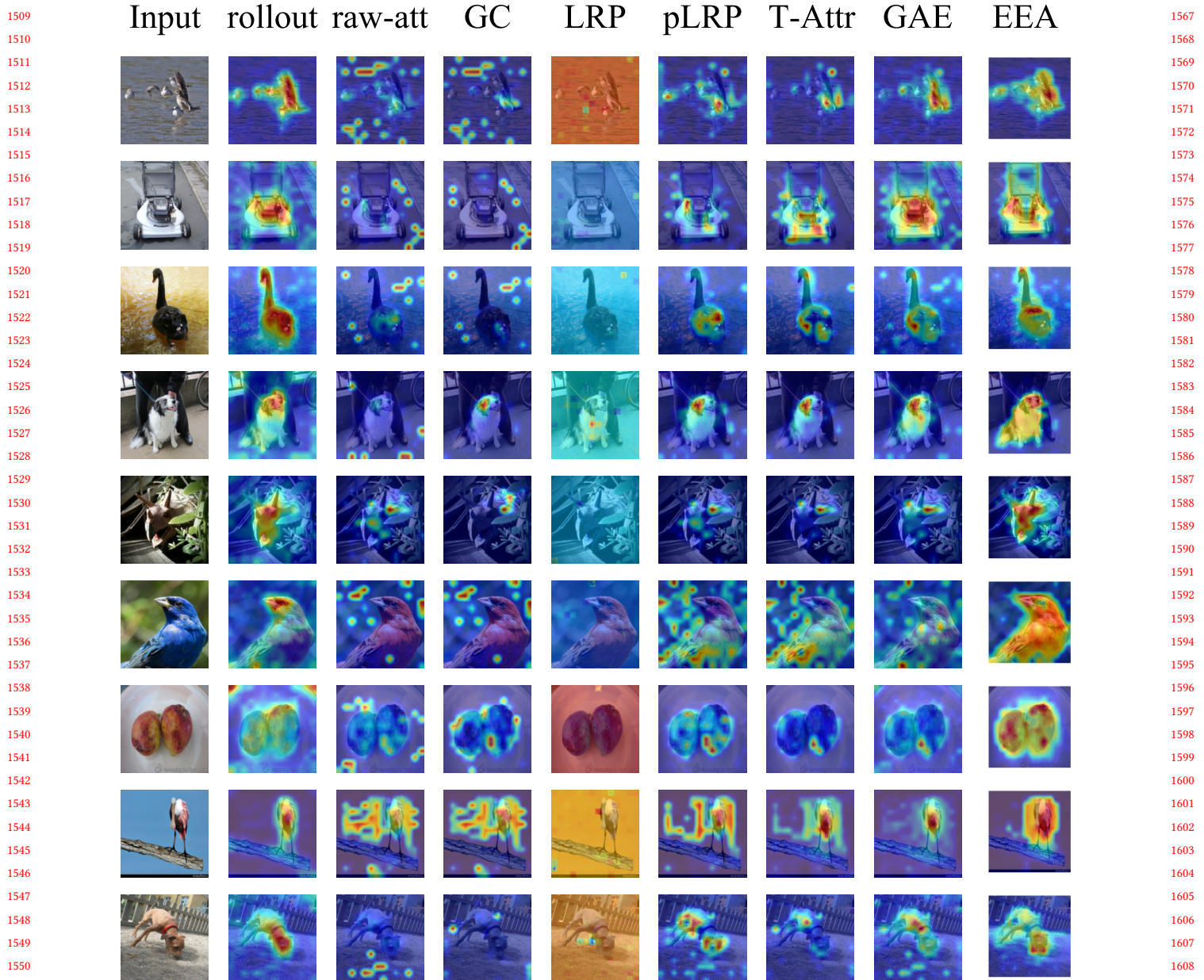
929
930
931
932
933
934
935
936
937
938
939
940
941
942
943
944
945
946
947
948
949
950
951
952
953
954
955
956
957
958
959
960
961
962
963
964
965
966
967
968
969
970
971
972
973
974
975
976
977
978
979
980
981
982
983
984
985
986
987
988
989
990
991
992
993
994
995
996
997
998
999
1000
1001
1002
1003
1004
1005
1006
1007
1008
1009
1010
1011
1012
1013
1014
1015
1016
1017
1018
1019
1020
1021
1022
1023
1024
1025
1026
1027
1028
1029
1030
1031
1032
1033
1034
1035
1036
1037
1038
1039
1040
1041
1042
1043
1044

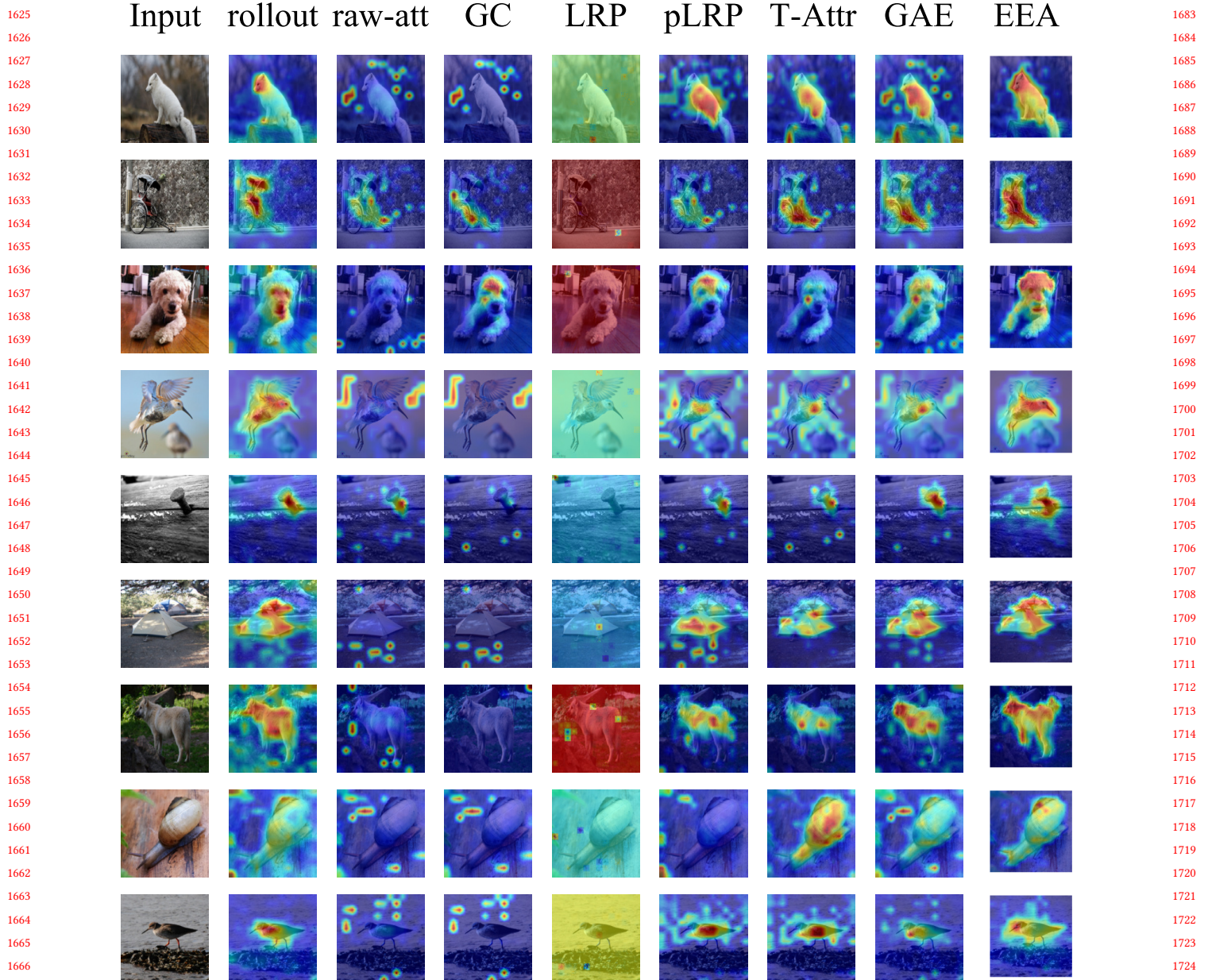












REFERENCES

- [1] Julius Adebayo, Justin Gilmer, Michael Muelly, Ian Goodfellow, Moritz Hardt, and Been Kim. 2018. Sanity checks for saliency maps. In *Advances in Neural Information Processing Systems*. 9505–9515.
- [2] Aditya Chattopadhyay, Anirban Sarkar, Prantik Howlader, and Vineeth N Balasubramanian. 2018. Grad-cam++: Generalized gradient-based visual explanations for deep convolutional networks. In *2018 IEEE winter conference on applications of computer vision (WACV)*. IEEE, 839–847.
- [3] Aditya Chattopadhyay, Anirban Sarkar, Prantik Howlader, and Vineeth N Balasubramanian. 2018. Grad-CAM++: Generalized Gradient-Based Visual Explanations for Deep Convolutional Networks. In *2018 IEEE Winter Conference on Applications of Computer Vision (WACV)*. 839–847. <https://doi.org/10.1109/WACV.2018.00097>
- [4] Hila Chefer, Shir Gur, and Lior Wolf. 2021. Transformer interpretability beyond attention visualization. In *Proceedings of the IEEE/CVF Conference on Computer Vision and Pattern Recognition*. 782–791.
- [5] Piotr Dabkowski and Yarin Gal. 2017. Real time image saliency for black box classifiers. In *Advances in Neural Information Processing Systems*. 6970–6979.
- [6] Vitali Petsiuk, Abir Das, and Kate Saenko. 2018. Rise: Randomized input sampling for explanation of black-box models. *arXiv preprint arXiv:1806.07421* (2018).